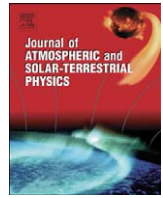




Contents lists available at ScienceDirect

Journal of Atmospheric and Solar-Terrestrial Physics

journal homepage: www.elsevier.com/locate/jastp

PFISR and ROPA observations of pulsating aurora

S.L. Jones^{a,*}, M.R. Lessard^a, P.A. Fernandes^a, D. Lummerzheim^b, J.L. Semeter^c, C.J. Heinselman^d,
K.A. Lynch^e, R.G. Michell^f, P.M. Kintner^g, H.C. Stenbaek-Nielsen^b, K. Asamura^h

^a Space Science Center, University of New Hampshire, Durham, NH 03824, USA

^b Geophysical Institute, University of Alaska - Fairbanks, Fairbanks, AK 99776, USA

^c Department of Electrical and Computer Engineering, Boston University, Boston, MA 02215, USA

^d SRI International, 333 Ravenswood Avenue, Menlo Park, CA 94025, USA

^e Department of Physics and Astronomy, Dartmouth College, Hanover, NH 03755, USA

^f Southwest Research Institute, 6220 Culebra Road, San Antonio, TX 78238, USA

^g Computer and Electrical Engineering, Cornell University, Ithaca, NY 14853, USA

^h Institute of Space and Astronautical Science, JAXA, Sagami-hara 229-8510, Japan

ARTICLE INFO

Article history:

Accepted 1 October 2008

Available online 21 October 2008

PACS:

94.20.Ac

94.20.wh

Vv 94.20

94.20.dg

94.20.dm

Keywords:

Pulsating aurora

Auroral thickness

Auroral ionosphere

PFISR

Sounding rocket

ROPA

ABSTRACT

Previous observations have shown that pulsating aurora sometimes occurs with patches of a vertical extent that is thinner than would be expected for aurora caused by collisional processes, implying that local ionospheric processes are important in causing the narrow luminosity enhancement. However, Poker Flat Incoherent Scatter Radar (PFISR) data from four pulsating aurora events, during the Rocket Observations of Pulsating Aurora (ROPA) mission in January and February 2007, show that the electron density profile associated with the pulsating patches had a thickness of ~15–25 km in all four cases and that, therefore, these are not examples of such thin enhancements. A numerical model of the associated volume emission rates for the night of the ROPA launch supports this conclusion. In the process of modeling the volume emission rates, the PFISR data are inverted to calculate the associated electron energy distribution for comparison with in situ electron measurements from ROPA and the REIMEI satellite. The modeled distribution shows a diffuse plasma sheet population which gradually decreases in energy over the course of the event, resulting in ~6–8 keV precipitation by the end of the PFISR data interval, in agreement with the ROPA/REIMEI measurements.

© 2008 Elsevier Ltd. All rights reserved.

1. Introduction

Time varying auroral displays involving more slowly varying structures, as opposed to rapid *motion*, are classified in the *International Auroral Atlas* (International Union of Geodesy and Geophysics (IUGG), 1963) as *pulsing* (not to be confused with *pulsating*), a term that encompasses a few different subclasses including those described below. One subclass is *pulsating* aurora which involves a quasi-periodic modulation of the intensity of extended forms with an average period of ~8 s (Royrvik and Davis,

1977). This is quite different from another subclass called *flickering* aurora, which tends to develop within discrete arcs and exhibits oscillations near 6–8 Hz and higher. *Flaming* aurora, while also an intensity modulation, is one that tends to travel upwards along local magnetic field lines. Finally, temporal changes in horizontal directions are classified as *streaming* if the motion appears to travel along an arc, or as *fast auroral waves* if the motion appears as a progression of arcs in latitude (Vallance Jones, 1974).

Pulsating aurora is typically observed to occur after auroral breakup in the post-midnight local time sector (Akasofu, 1968; Duthie and Scourfield, 1977). However, a study of 34 nights by Oguti et al. (1981) shows that the occurrence probability for pulsating aurora increases to ~100% after 0400 MLT and that morningside pulsating aurora can occur even during times of low magnetic activity. In contrast with breakup aurorae, which tend to exhibit narrow, discrete arcs with significant east–west extent, pulsating aurora appears as a series of patches, typically embedded in a diffuse background aurora or, occasionally, in a weak auroral display extended in the east–west directions. Typical

* Corresponding author. Tel.: +1 603 862 1391; fax: +1 603 862 0311.

E-mail addresses: sarah.jones@unh.edu (S.L. Jones),

marc.lessard@unh.edu (M.R. Lessard),

philip.fernandes@alumni.unh.edu (P.A. Fernandes),

lumm@gi.alaska.edu (D. Lummerzheim), jls@bu.edu (J.L. Semeter),

craig.heinselman@sri.com (C.J. Heinselman),

kristina.lynch@dartmouth.edu (K.A. Lynch),

rmichell@swri.edu (R.G. Michell), pmk1@cornell.edu (P.M. Kintner),

hnielsen@gi.alaska.edu (H.C. Stenbaek-Nielsen),

asamura@stp.isas.jaxa.jp (K. Asamura).

periods of pulsations range from a few seconds to a few 10s of seconds, and sizes range from 10 to 200 km in horizontal extent (Royrvik and Davis, 1977; Oguti, 1978; Yamamoto, 1988). Duncan et al. (1981), using results from seven nights of observing, determined that 0.1–100 s periods were possible, but note that they observed periods between 5 and 10 s for two-thirds of their observations.

In addition to having the characteristic patch structure described above, pulsating aurora is often observed against a non-pulsating background (Royrvik and Davis, 1977; Stenbaek-Nielsen and Hallinan, 1979), presumably created by primary soft electron precipitation (Smith et al., 1980; McEwen et al., 1981; Sandahl, 1985). However, it has also been suggested by Evans et al. (1987) that the diffuse auroral background may be an intrinsic feature of pulsating aurora, with at least some component of this steady, soft precipitation “created as a natural consequence of a time-variable primary precipitation” arising from secondary and backscattered electrons.

Excellent reviews of pulsating aurora have been presented by Davis (1978), Johnstone (1978, 1983), Sandahl (1985) and Davidson (1990). It is generally believed that pulsating aurora is caused by energetic electrons (Smith et al., 1980; McEwen et al., 1981) precipitated by pitch-angle diffusion in the vicinity of the equatorial region of the magnetosphere (Yau et al., 1981; Davidson, 1986a, b; Huang et al., 1990), a result based on velocity dispersion analyses of sounding rocket observations of energetic electrons in conjunction with pulsating aurora. However, note that a lack of velocity dispersion in the energetic particle measurements has been shown in some instances (Johnstone, 1971; Williams et al., 2006).

Also supporting an equatorial source region are observations of magnetically conjugate pulsating auroras (Belon et al., 1969; Davis, 1978; Gokhberg et al., 1970). However, several optical studies have shown a lack of conjugacy for pulsating auroras, with pulsating aurora sometimes occurring in one hemisphere but not the other, or with conjugate auroras that are not pulsating in phase (Minatoya et al., 1995; Sato et al., 1998, 2002, 2004; Watanabe et al., 2007). Sato et al. (2004) suggest that in these instances, although the particles probably originate near the equatorial magnetosphere, there may be a near-Earth modulation source.

Davidson (1990) states that rocket and satellite measurements of the electron precipitation associated with pulsating aurora show the characteristic energy to be highly variable from one event to the next, with characteristic energies ranging from several keV to several 10s of keV, but that “the pulsating component is negligible or very small below about 2–4 keV.” However, McEwen et al. (1981) report several instances of morningside pulsating aurora caused by precipitating electrons with Maxwellian distributions of unexpectedly low average energy (as low as 1.5–1.8 keV over a pulsation period), and thus they conclude that *morningside* pulsating aurora may, in fact, be caused by low energy electrons.

Some questions arise with regard to the thickness of the pulsating patches. Störmer (1948) showed results from a statistical study of 12,330 measurements acquired in Norway. Although he did not specifically address the thickness of individual patches, he did show that the upper limit (in altitude) of pulsating aurora was typically near 110 km, with a lower limit near 90 km. More recent observations were reported by Stenbaek-Nielsen and Hallinan (1979), who concluded that patches are often as thin as ~2 km or less. Such thin pulsating auroral patches are much thinner than can be explained by collisional thermalization, even for a monoenergetic, monodirectional beam, indicating the existence of a process internal to the ionosphere (Stenbaek-Nielsen and Hallinan, 1979). Subsequent

observations have shown pulsating patches with significant vertical extent (Hallinan et al., 1985), suggesting that the thin pulsating patches observed by Stenbaek-Nielsen and Hallinan (1979) are a subset of pulsating aurora.

Such thin layers have been observed (Donahue et al., 1968; Oguti, 1975; Mishin et al., 1981; Hallinan et al., 1985) in many auroral forms, including discrete arcs. These layers are of negligible vertical extent (often <1 km) and have been termed *enhanced aurora* (Hallinan et al., 1985). One proposed explanation is that these luminosity enhancements are created by excitations due to a local suprathermal electron population resulting from wave-particle interactions, with wave growth taking energy from the incident auroral precipitation (Hallinan et al., 1997; Johnson, 2006). However, the exact process remains to be determined.

Previous observations of pulsating aurora using EISCAT in Tromsø, Norway, directed towards Kilpisjärvi, Finland (ILAT = 66°) were presented by Kaila et al. (1989), Kaila and Rasinkangas (1989), and Böisinger et al. (1996). A pulsating arc was observed with two distinct modulations of 10 and 60 s periods. The EISCAT data for this event show two peaks in electron density (at 95 and 115 km altitude), the lower of which occurs over ~8 km (Kaila and Rasinkangas, 1989, Figs. 4 and 5; Böisinger et al., 1996, Figs. 5 and 6). Note that the EISCAT perspective for these observations is not field aligned. Böisinger et al. (1996) infer a double Maxwellian electron distribution, with the higher energy peak likely causing the pulsations with 10 s periods. Wahlund et al. (1989) report similar EISCAT observations showing single, and in some cases double (at approximately 108 and 123 km altitude), thin layers in the ionospheric electron density of <4.5 km thickness in support of the Stenbaek-Nielsen and Hallinan (1979) results.

In this study, the question of patch thickness is addressed from the perspective of Poker Flat Incoherent Scatter Radar (PFISR) and the Rocket Observations of Pulsating Aurora (ROPA) sounding rocket and REIMEI satellite observations, supported with numerical analysis.

2. ROPA campaign

The ROPA campaign took place in January/February 2007, at the Poker Flat Research Range (65.1°, 212.5° geographic) near Fairbanks, AK. The objective of the campaign was to study various aspects of pulsating aurora, with the use of a sounding rocket and a complete suite of ground instruments, including the newly developed PFISR.

During the campaign, several instances of pulsating aurora were observed and recorded with intensified video cameras. In this paper, we show data from four examples (from four different nights) that had good optical data, as well as good PFISR data. The particular example associated with the ROPA launch, which occurred at 1245 UT (~0141 MLT) on February 12, 2007, is presented and discussed in detail.

The pulsating aurora event on the night of the ROPA launch developed out of diffuse aurora which began to form at ~1119 UT (0015 MLT) after a substorm breakup with pulsations starting at ~1122 UT. Preliminary analysis of Poker Flat all-sky camera (ASC) data (white light) shows patches which are often east-west elongated, including some pulsating arc segments, spanning up to 10s of km. Plotting optical intensity from the Poker Flat ASC (see Fig. 1) at two frames per second, summed over 0.03° latitude and 0.1° longitude around the point where the PFISR beam intersects ~100–110 km altitude (64.95°, 212.33° geographic), we see simultaneous modulations of approximately 6 and 20 s periods. The event lasted for just over 2 h, gradually weakening in intensity over the duration. The pulsating aurora extended over roughly 65–67° ILAT, or from just south of Poker Flat to just north of Fort

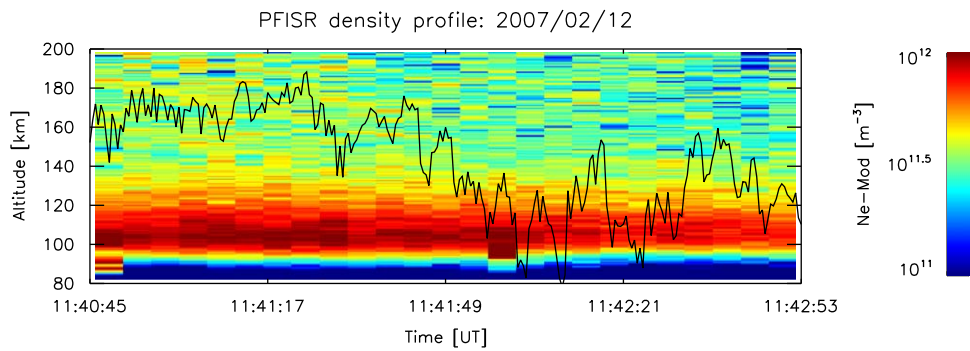


Fig. 1. Plot shows the electron density measured by PFISR on February 12, 2007. Overplotted is the auroral brightness from the Poker Flat all-sky camera (2 frames per second) in arbitrary units. The values are summed over 0.03° latitude and 0.1° longitude around the point where the PFISR beam intersects ~ 100 – 110 km altitude (64.95° , 212.33° geographic). Note the modulations in brightness of approximately 6 and 20 s periods.

Yukon, AK. The ROPA sounding rocket measurements were taken from near the poleward edge of this region and northward throughout the rocket flight (from 1245 to 1259 UT).

Fig. 1 clearly shows that the time resolution of the PFISR measurements (~ 5 s) is not high enough to distinguish the pulsating behavior for the February 12 event (~ 6 s). Therefore, the PFISR data analysis provides averages over the pulsation “on” and “off” phases. This information is supplemented with higher time resolution data from ground based optics and in situ particle detectors. Note that the PFISR beam used in this study consists of a $480 \mu\text{s}$ long pulse interleaved with a 13 baud ($10 \mu\text{s}$) Barker code on two frequencies, allowing better than 1 km altitude resolution over the 50–200 km altitude range.

Fig. 2 shows ionospheric electron density enhancements measured by PFISR for four pulsating aurora events, with pulsating aurora occurring over the duration of the four data sets. The plots show more intense density enhancements early on in the pulsating events, with the density peak of these enhancements varying in altitude (see Fig. 3a) from one event to the next (near 83 km at the start of the first and second events and closer to 95 and 110 km for the third and fourth events). For the January 17–18 and February 12 events, the density peak had clearly increased in altitude (i.e. the bulk of the precipitation had softened) by the end of the data set. Note that on February 12 the rocket was not launched before this time because the poleward edge of the pulsating aurora had not migrated far enough north to be under the trajectory of the rocket (to the north of Poker Flat).

By performing a Gaussian fit to the density profiles for the four events (see Fig. 3b), we find a FWHM of ~ 15 – 25 km which is several times greater than the vertical extent of the thin patches observed by Wahlund et al. (1989) using EISCAT and seems consistent with a density profile caused by standard collisional processes.

2.1. Numerical estimate of incident electron energy spectrum

We concentrate on the fourth event in order to compare with ROPA electron observations. PFISR observations of density profiles can be inverted to estimate the primary electron distribution. The procedure used here is described in detail by Semeter and Kamalabadi (2005) and uses a forward model based on the Rees (1963) approach. In this instance, the pitch-angle distribution in the downward hemisphere is assumed to be isotropic (a fairly good assumption for pulsating aurora).

It is important to note that this model assumes that collisional processes are responsible for the enhanced electron density

measured by PFISR. Therefore, the resulting inversion will not be valid if local ionospheric processes such as wave–particle interactions are important to the creation of pulsating patches. Such noncollisional processes have been proposed as a possible cause of the extremely thin patches observed by Stenbaek-Nielsen and Hallinan (1979) and Wahlund et al. (1989). If noncollisional processes are important to the events analyzed here, we would expect that either the inversion will not converge to a solution or that the solution will not be able to reproduce the observed ionospheric electron density profile and/or will differ significantly from in situ particle measurements.

Of the sources of uncertainty detailed in Semeter and Kamalabadi (2005), the most important in this case is the neutral atmosphere model (MSIS-90) because the neutral composition can stray from predictions due to the presence of aurora. However, changes in the neutral composition tend to take place on a longer timescale than changes in the aurora, producing a mostly systematic error in the inverted energy spectra as for the February 12 inversion discussed below.

Fig. 4 shows the differential energy flux ($\text{cm}^2 \cdot \text{s} \cdot \text{sr} \cdot \text{eV/eV}^{-1}$) of precipitating electrons computed via inversion of PFISR measurements. In the bottom panel of Fig. 2 a decrease in electron density at higher altitudes (> 140 km) can be seen shortly after the start of the data interval, which clearly corresponds with a decrease in the flux of lower energy (< 1 keV) electrons estimated by the inversion for the same time period.

The numerical estimate (from inversion of PFISR data) of differential energy flux (see Fig. 4) shows that the inversion frequently results in two peaks in the distribution. Fig. 5b shows a line plot of differential number flux from the numerical inversion for February 12 at 1141.55 UT, approximately 1 h before the ROPA launch. The inversion estimates two peaks in the electron distribution at this time; at 6 and 20 keV. Such results should be treated with caution, since the appearance of multiple peaks is a common artifact of the inversion procedure. However, some evidence that this is a meaningful result is found in Fig. 5a, which shows the PFISR measured density profile (solid line), with the estimated density profile calculated from the inverted electron distribution shown in Fig. 5b (dashed line). A high energy population is manifested as an ionization enhancement at low altitudes, in the bottomside of the auroral E-region. Note that there is an enhancement below 90 km that is not well reproduced by the inversion (dashed line). It is likely that this lower altitude enhancement results in the 20 keV population estimated by the inversion. Thus the presence of this higher energy peak corresponds to a clear feature in the measured plasma density and is likely the signature of the pulsation “on” phase. Improving the fit in the 85–90 km range would involve increasing the flux of

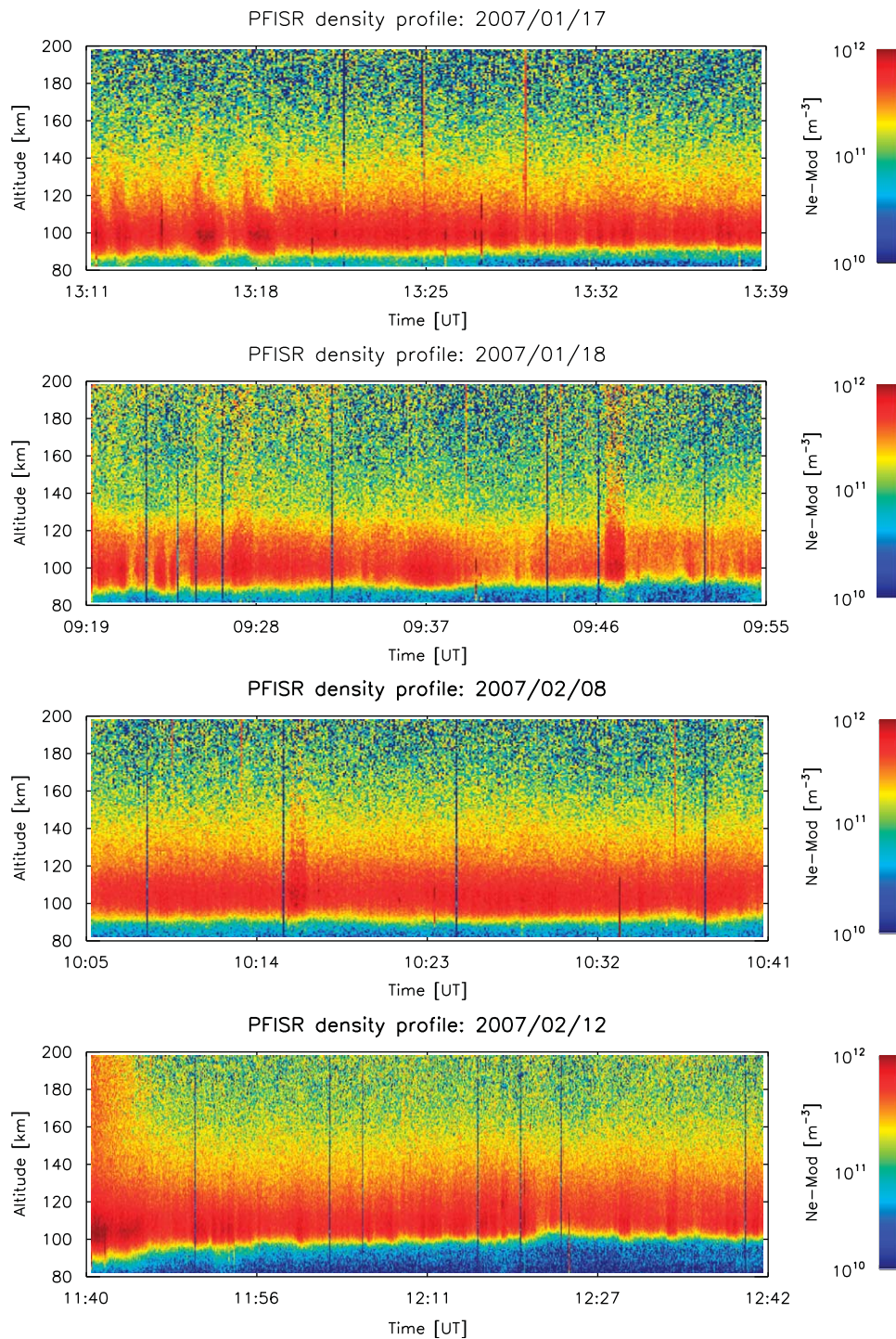


Fig. 2. Plots show the electron density measured by PFISR for four pulsating aurora events: January 17–18, February 8 and February 12, 2007. Note that the altitude of the density maximum varies from one event to another.

primaries in the range of 23–49 keV (see Semeter and Kamalabadi, 2005, Fig. 2) by increasing the energy of the second peak in the distribution.

The result of the inversion can be compared with the precipitating electron energy distribution measured by the ROPA electron hemispherical electrostatic energy and pitch angle spectrometer (HEEPS), which has an energy range of approximately 0.01–20 keV. Fig. 6 shows the measured differential energy flux ($\text{cm}^2 * \text{s} * \text{sr} * \text{eV}/\text{eV}^{-1}$) of precipitating electrons, corresponding to the period of time from 1247:44 to 1249:44 UT.

During this period of time, the ROPA payload was north of PFISR in the vicinity of the poleward edge of the pulsating aurora near Fort Yukon, AK.

Electrostatic analyzer (ESA) measurements from the REIMEI satellite (see Fig. 7) taken during the PFISR data interval, and within the field-of-view of the Poker Flat ASC, show this to be a downgoing population and therefore primary precipitation, or perhaps secondary electrons from the conjugate hemisphere (Sato et al., 2002, 2004) or downward accelerated secondary electrons such as those observed by Williams et al. (2006).

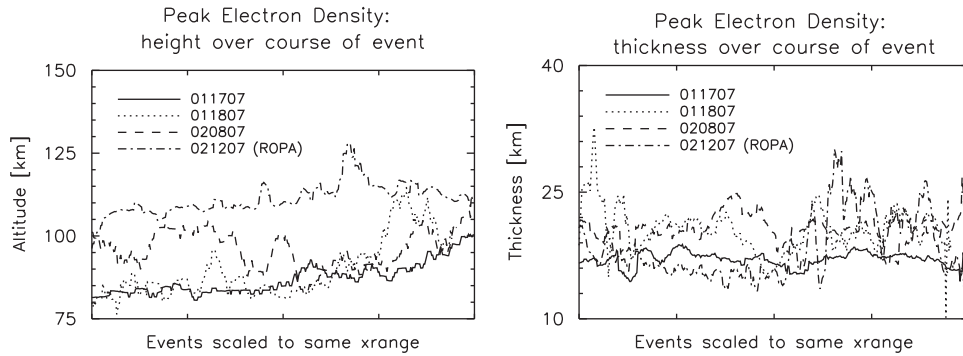


Fig. 3. Plots show evolution of the electron density peak over the four events, which are scaled to the same x-range. The altitude (left) and vertical extent (right) of the peak ionospheric electron density are obtained from a Gaussian fit.

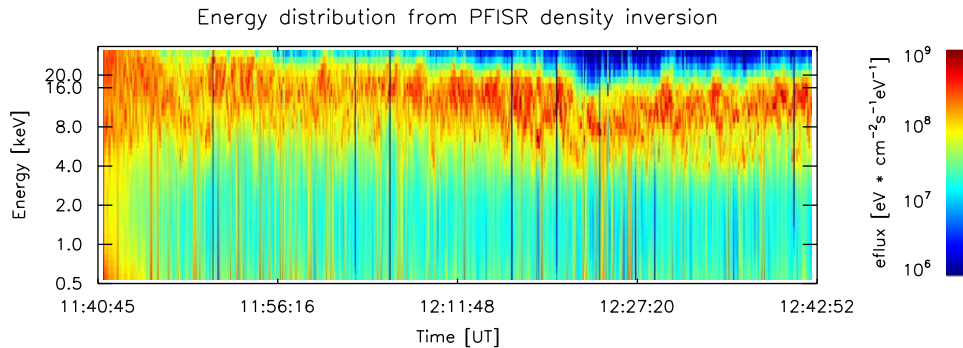


Fig. 4. Plot shows differential energy flux ($\text{cm}^2 * \text{s} * \text{str} * \text{eV}/\text{eV}^{-1}$) of precipitating electrons calculated via inversion of the PFISR electron density profiles over an energy range of 0.5–32.5 keV for the February 12, 2007 event.

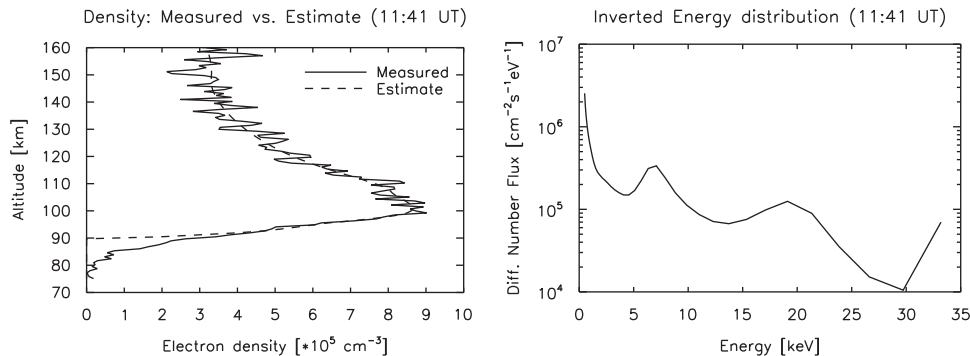


Fig. 5. Plot (a) shows altitude vs. measured electron density profile (solid line) from the PFISR data, with the calculated density profile (dashed line) from the numerical estimate of the associated electron distribution obtained by inversion of the PFISR data; shown in plot (b).

Fig. 8 is a plot of the same measurements taken by the HEEPS onboard the ROPA fly-away detector (FAD) subpayload. FAD1 was ejected eastward from the main payload and therefore had better optical coverage. Superimposed on the figure is a line plot of the auroral brightness taken from the Fort Yukon ASC showing modulations with roughly the same period as seen in Fig. 1.

Direct comparison of the differential energy flux from inversion of PFISR vs. the in situ measurements shows that the inversion does overestimate the values as mentioned above, presumably due to the model of neutral atmospheric composition. However, it is clear that the inversion recovers the ~ 6 keV population as well as intermittent < 1 keV precipitation and therefore provides a useful estimate of the differential energy flux associated with pulsating aurora.

2.2. Numerical estimate of luminosity profile

We can use the precipitating electron distribution function obtained by the above PFISR inversion method as model input to numerically estimate the associated auroral luminosity profile. The transport of energetic electrons into the atmosphere can be described with a Boltzmann equation that equates the change in the electron-distribution function in a given phase-space volume to the changes in moving to a different altitude, changing the direction in elastic scattering, changing the energy in inelastic scattering, and the production of secondary electrons in ionizing collisions. Here we use the model of Lummerzheim and Liliensten (1994), which uses the discrete-ordinate method to solve the energy degradation and electron transport problem and uses a multi-stream approach

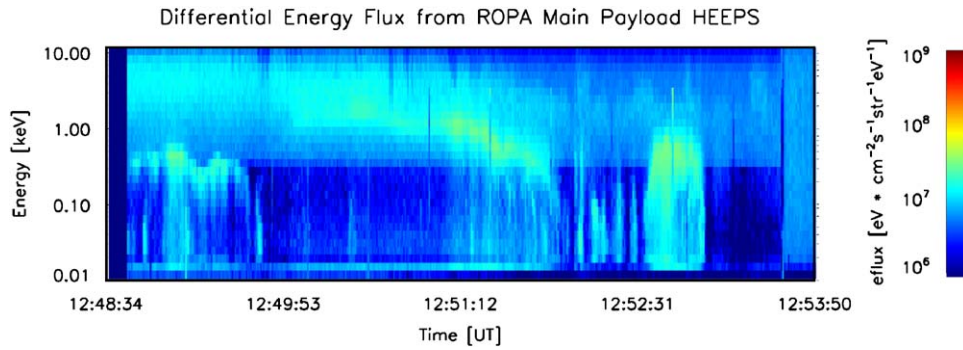


Fig. 6. Plot shows electron differential energy flux ($\text{cm}^2 * \text{s} * \text{str} * \text{eV}/\text{eV}^{-1}$) measured by the ROPA HEEPS from 220 to 245 s into launch, near the poleward boundary of the pulsating aurora. Note the peak in energy at ~ 6 keV as well as the intermittent population at ~ 300 eV. Fluxes are slightly underestimated due to assumption of an isotropic distribution.

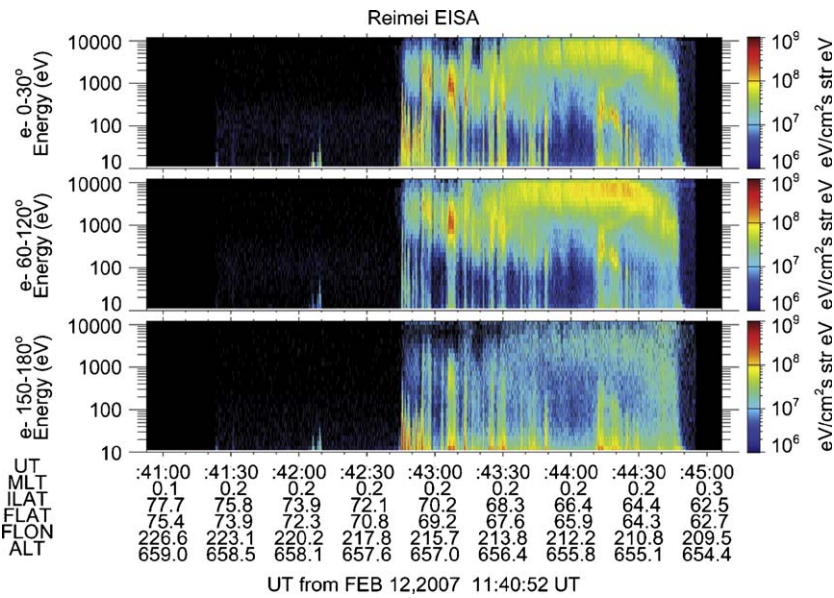


Fig. 7. Plot shows electron differential energy flux ($\text{cm}^2 * \text{s} * \text{str} * \text{eV}/\text{eV}^{-1}$) measured by the REIMEI ESA as the satellite moved poleward across Poker Flat, AK. Note the peak in energy at ~ 6 keV as well as the downgoing, intermittent population at < 1 keV, similar to measurements made by ROPA HEEPS approximately 1 h later during the same pulsating aurora event.

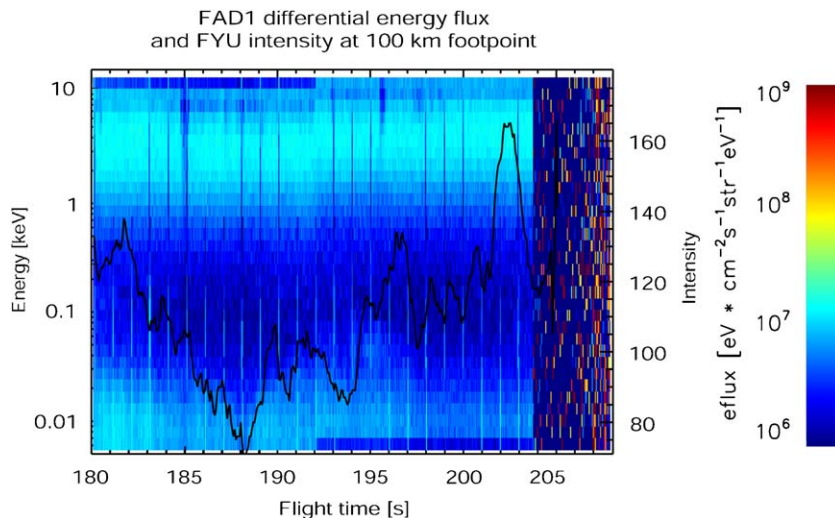


Fig. 8. Plot shows electron differential energy flux ($\text{cm}^2 * \text{s} * \text{str} * \text{eV}/\text{eV}^{-1}$) measured by the ROPA FAD1 HEEPS from 180 to 205 s after launch (1148:04–1148:29 UT), near the poleward boundary of the pulsating aurora. Overplotted is the auroral brightness at the footprint of the FAD1 subpayload from the Fort Yukon all-sky camera (30 frames per second, smoothed to reduce intensifier noise) in arbitrary units. Fluxes are slightly underestimated due to assumption of an isotropic distribution.

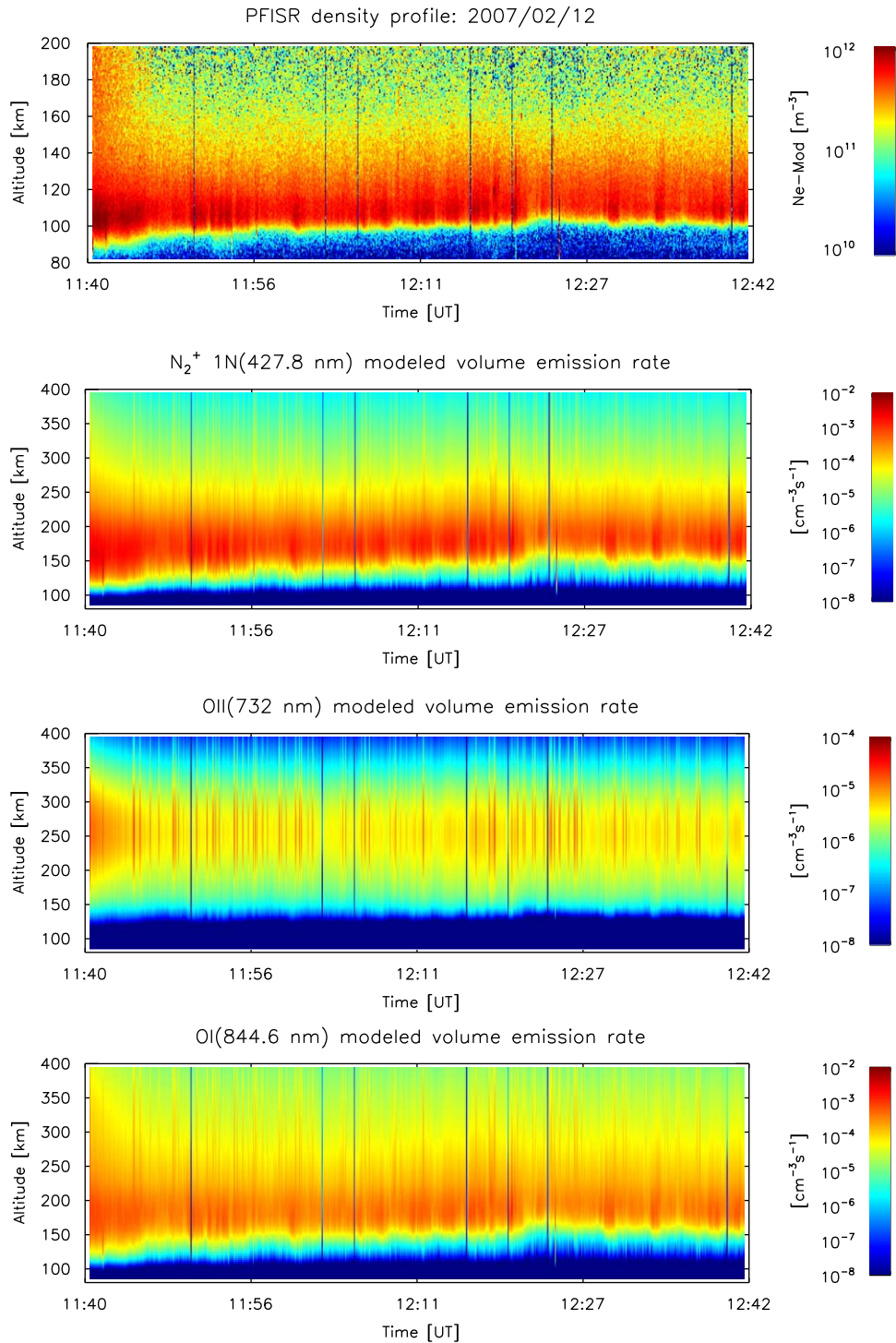


Fig. 9. Top panel shows the electron density profile measured by PFISR for the night of the ROPA launch. Bottom three panels show the corresponding numerical estimates of volume emission rates calculated from numerical inversion of PFISR data for three auroral emissions: 427.8, 732, and 844.6 nm.

to solve for the electron intensity as a function of energy and altitude.

This model was used to estimate volume emission rates ($\text{cm}^{-3}\text{s}^{-1}$) for three auroral emissions: the N₂⁺ 1neg (427.8 nm) emission, with an emission rate that is directly proportional to the ionization rate; the OI(844.6 nm) emission, with two excitation sources (direct excitation of O and dissociative excitation of O₂) leading to low and high altitude contributions to the emission profile; and the OII(732.0 nm) emission which, in part due to

quenching at lower altitudes, provides an indication of lower energy precipitation.

The emissions of the N₂⁺ 1neg (427.8 nm) and the OI(844.6 nm) are prompt emissions and are calculated directly from the excitation rate. No cascade contributions are considered, but the OI(844.6 nm) has contributions from direct excitation of atomic oxygen and dissociation of molecular oxygen. The OII(732.0 nm) emission results from the excited O⁺(2P) state. Electron impact ionization of atomic oxygen yields about 18% O⁺(2P) ions.

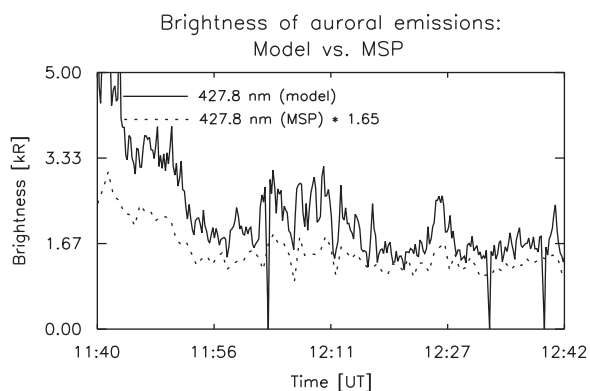


Fig. 10. Plot shows brightness (kR) vs. time (UT) calculated from model estimates of the volume emission rate for the 427.8 nm auroral emission and the measured brightness from Poker Flat MSP data (102° look-angle; intersecting PFISR beam at 100 km altitude) in 427.8 nm for the ROPA event. Note that the MSP data is multiplied by 1.65 to account for scattering and extinction in the atmosphere.

Deactivation of the excited state occurs through quenching with N_2 and O as well as emission of a photon (Lummerzheim et al., 1990). The continuity equation governing the ion chemistry of the $O^+(2P)$ is solved with a quasi static assumption, which is justified by the time resolution of our data.

Fig. 9 shows volume emission rates for the above emissions for the ROPA event calculated using the numerical model. The top panel is a plot of the PFISR electron density measurements for comparison. We can see that the 427.8 and 844.6 nm emissions closely match the density profile, with more intense features in the density profile clearly visible as enhancements in the volume emission rates. The volume emission rate at 732.0 nm is approximately two orders of magnitude less intense than the above mentioned emissions, with the emissions quenched below an altitude of ~ 150 km.

Fig. 10 shows the brightness (kR) of the 427.8 nm emission, calculated from the modeled volume emission rates. The Poker Flat meridian scanning photometer (MSP) data for 427.8 nm (102° look-angle intersecting PFISR beam at 100 km altitude) is plotted for comparison. The MSP measurements are multiplied by a correction factor to account for scattering and extinction in the atmosphere (1.65 for 427.8 nm along the zenith with clear sky at Poker Flat (Lummerzheim et al., 1990)). Note that although the model overestimates the brightness (due to overestimating the fluxes from the PFISR inversion) the shape of the curve agrees quite well with the MSP curve, with 16 s between samples due to the scanning of the photometer. This suggests that the numerical model, used in conjunction with the numerical inversion of the PFISR data, provides a good estimate of the associated emission rates.

3. Discussion and conclusions

Comparison of the modeled precipitating electron energy flux (Semeter and Kamalabadi, 2005) with in situ particle measurements for the night of the ROPA launch suggests that the inverted distribution is a good estimate of the electron precipitation associated with pulsating aurora. The modeled distribution can then be used as input to an electron transport and ionospheric model to calculate the corresponding emission rate profiles (Lummerzheim and Liliensten, 1994) for selected emissions, which can be integrated to provide the brightness for each emission for comparison with optical observations. Comparing the modeled brightness to the Poker Flat MSP measurements at 427.8 nm for

the ROPA event shows agreement. Therefore, through the use of these two models, it is possible to obtain an approximate measure of the precipitating electron distribution and luminosity from PFISR measurements. This type of analysis will be useful for a wide variety of projects.

The ionospheric electron density profiles for the four events are shown to have a thickness of ~ 15 – 25 km (FWHM), suggesting that none of these instances of pulsating aurora are examples of the unusually thin patches observed by Stenbaek-Nielsen and Hallinan (1979) and Wahlund et al. (1989).

The PFISR inversion from before the ROPA launch shows a gradual decrease in energy of the higher energy precipitating electron population resulting in lower energy (~ 6 – 8 keV) precipitation by the end of the PFISR measurements. The inversion also reproduces an approximately 6 keV diffuse population which was measured in situ by both REIMEI (during the PFISR interval) and ROPA (shortly afterward).

We see from the PFISR density profiles for four events (January 17 and 18, February 8 and 12) that the electron energies vary slightly from one event to the next, as evidenced by slight variations in the altitude of the peaks in ionospheric electron density and volume emission rate. Also, for three of the four events (January 17 and 18 and February 12), the electron precipitation softens over the course of the event with a gradual increase in the altitude of the peak in electron density. For the ROPA event (February 12), we see a corresponding decrease in energy of the higher energy precipitation, as estimated by the numerical model.

The presence of lower energy (< 1 keV) precipitation (Fig. 5), shown via inversion of the PFISR data, is most intense at the beginning of the radar data interval (~ 1140 UT) after which it appears sporadically. This precipitation is likely responsible for the electron density enhancement at higher altitudes, seen in Fig. 2 at the beginning of the ROPA event. Intermittent, low energy precipitation is also measured in this region by ROPA and REIMEI (downgoing) during the February 12 event, and appears to be primary electron precipitation which may (Sato et al., 2002, 2004) or may not be related to pulsating aurora.

Poker Flat ASC images (not shown) for the four events chosen show the development of diffuse aurora directly preceding the pulsating aurora, with patchy structure gradually forming within a region of diffuse aurora and, on a timescale of minutes, beginning to pulsate. In fact, the observations suggest that the presence of diffuse aurora is a necessary precursor for the development of pulsating aurora. It has been suggested by Stenbaek-Nielsen (1980) and Evans et al. (1987) and many others that there may be an important relationship between pulsating and diffuse aurora. Our observations support this suggestion, showing a time ordered relationship between the two phenomena.

The main conclusions of the paper are as follows:

- (1) The chosen events do not show the thin enhancements seen by Stenbaek-Nielsen and Hallinan (1979) and Wahlund et al. (1989) associated with pulsating aurora. This supports the conclusion of Hallinan et al. (1985) that such thin patches are a subset of pulsating aurora.
- (2) There is a large amount of variability in the altitude of the peak ionospheric electron density enhancement due to pulsating aurora, both from one event to the next and over the course of a single event, suggesting a corresponding variability in the energy distribution of incident electrons causing the pulsating aurora. For the ROPA event, the estimated higher energy precipitation showed a gradual decrease in energy, which coincided with a gradual weakening in the pulsating aurora.

(3) During the ROPA mission, ASC observations often showed diffuse aurora preceding pulsating aurora, with patches developing within the diffuse aurora and over time beginning to pulsate. For the February 12 event, measured and calculated precipitating electron distributions show the pulsating aurora collocated with widespread diffuse aurora. Thus, it seems likely that the presence of diffuse aurora is a requirement for the development of pulsating aurora.

Acknowledgments

Research at the University of New Hampshire, Cornell University, Dartmouth College, and by Stenbaek-Nielsen and Lummerzheim at the University of Alaska—Fairbanks was supported by NASA Grants NNG05WC36G, NNG05WC37G, NNG05WC38G, and NNG05WC39G, respectively. Work at Boston University was supported by NSF Grant ATM-0538868, and PFISR data collection and analysis were supported by NSF Grant ATM-0608577.

References

- Akasofu, S.I., 1968. Polar and Magnetospheric Substorms. D. Reidel, Dordrecht, Holland, p. 223.
- Belon, A.E., Maggs, J.E., Davis, T.N., Mather, K.B., Glass, N.W., Hughes, G.G., 1969. Conjugacy of visual aurora during magnetically quiet periods. *Journal of Geophysics Research* 74, 1–28.
- Bösinger, T., Kaila, K., Rasinkangas, R., Pollari, P., Kangas, J., Trakhtengerts, V., Demekhov, A., Turunen, T., 1996. An EISCAT study of a pulsating auroral arc: simultaneous ionospheric electron density, auroral luminosity and magnetic field pulsations. *Journal of Atmospheric and Terrestrial Physics* 58, 23–35.
- Davidson, G.T., 1986a. Pitch angle diffusion in morningside aurorae 2. The formation of repetitive auroral pulsations. *Journal of Geophysical Research* 91, 4429–4436.
- Davidson, G.T., 1986b. Pitch angle diffusion in morningside aurorae. I—The role of the loss cone in the formation of impulsive bursts of precipitation. II—The formation of repetitive auroral pulsations. *Journal of Geophysical Research* 91, 4413–4427.
- Davidson, G.T., 1990. Pitch–Angle diffusion and the origin of temporal and spatial structures in morningside aurorae. *Space Science Reviews* 53, 45.
- Davis, T.N., 1978. Observed characteristics of auroral forms. *Space Science Reviews* 22, 77.
- Donahue, T.M., Parkinson, T., Zipf, E.C., Doering, J.P., Fastie, W.G., Miller, R.E., 1968. Excitation of the auroral green line by dissociative recombination of the oxygen molecular ion: analysis of two rocket experiments. *Planetary and Space Science* 16, 737.
- Duncan, C.N., Creutzberg, F., Gattinger, R.L., Harris, F.R., Vallance Jones, A., 1981. Latitudinal and temporal characteristics of pulsating auroras. *Canadian Journal of Physics* 59, 1063–1069.
- Duthie, D.D., Scourfield, M.W.J., 1977. Aurorae and closed magnetic field lines. *Journal of Atmospheric and Terrestrial Physics* 39, 1429–1434.
- Evans, D.S., Davidson, G.T., Voss, H.D., Imhof, W.L., Mobilia, J., Chiu, Y.T., 1987. Interpretation of electron spectra in morningside pulsating aurorae. *Journal of Geophysical Research* 92, 12295.
- Gokhberg, M.B., Kazak, B.N., Raspopov, O.M., Roldugin, V.K., Troitskaya, V.A., Fedoseyev, V.I., 1970. Pulsating auroras at conjugate points. *Geomagnetism and Aeronomy* 10, 289.
- Hallinan, T.J., Kimball, J., Stenbaek-Nielsen, H.C., Deehr, C.S., 1997. Spectroscopic evidence for suprathermal electrons in enhanced auroras. *Journal of Geophysical Research* 102, 7501–7508.
- Hallinan, T.J., Stenbaek-Nielsen, H.C., Deehr, C.S., 1985. Enhanced aurora. *Journal of Geophysical Research* 90, 8461–8475.
- Huang, L., Hawkins, J.G., Lee, L.C., 1990. On the generation of the pulsating aurora by the loss cone driven whistler instability in the equatorial region. *Journal of Geophysical Research* 95, 3893–3906.
- Johnson, J.R., 2006. Localization of the enhanced aurora and heavy ion ionization layers. AGU Fall Meeting Abstracts, B289, December 2006.
- Johnstone, A.D., 1971. Correlation between electron and proton fluxes in postbreakup aurora. *Journal of Geophysical Research* 76, 5259.
- Johnstone, A.D., 1978. Pulsating aurora. *Nature* 274, 119–126.
- Johnstone, A.D., 1983. The mechanism of pulsating aurora. *Annales Geophysicae* 1, 397–410.
- Kaila, K.U., Rasinkangas, R.A., 1989. Coordinated photometer and incoherent scatter radar measurement of pulsating arcs with high time resolution. *Planetary and Space Science* 37, 545–553.
- Kaila, K.U., Rasinkangas, R.A., Pollari, P., Kuula, R., Kangas, J., 1989. High resolution measurements of pulsating aurora by EISCAT, optical instruments and pulsation magnetometers. *Advances in Space Research* 9, 53–56.
- Lummerzheim, D., Liliensten, J., 1994. Electron transport and energy degradation in the ionosphere: evaluation of the numerical solution, comparison with laboratory experiments and auroral observations. *Annales Geophysicae* 12, 1039.
- Lummerzheim, D., Rees, M.H., Romick, G.J., 1990. The application of spectroscopic studies of the aurora to thermospheric neutral composition. *Planetary and Space Science* 38, 67–78.
- McEwen, D.J., Yee, E., Whalen, B.A., Yau, A.W., 1981. Electron energy measurements in pulsating auroras. *Canadian Journal of Physics* 50, 1106.
- Minatoya, H., Sato, N., Saemundsson, T., Yoshino, T., 1995. Absence of correlation between periodic pulsating auroras in geomagnetically conjugate areas. *Journal of Geomagnetism and Geoelectricity* 47, 583–598.
- Mishin, E.V., Ivchenko, V.N., Milinevskii, G.P., 1981. Fine structure of artificial auroral rays. *Advances in Space Research* 1, 163–165.
- Oguti, T., 1975. Two-tiered auroral band. *Journal of Atmospheric and Terrestrial Physics* 37, 1501–1504.
- Oguti, T., 1978. Observations of rapid auroral fluctuations. *Journal of Geomagnetism and Geoelectricity* 30, 299.
- Oguti, T., Kokubun, S., Hayashi, K., Tsuruda, K., Machida, S., Kitamura, T., Saka, O., Watanabe, T., 1981. Statistics of pulsating auroras on the basis of all-sky TV data from five stations. I. Occurrence frequency. *Canadian Journal of Physics* 59, 1150–1157.
- Rees, M.H., 1963. Auroral ionization and excitation by incident energetic electrons. *Planetary and Space Science* 11, 1209.
- Royrvik, O., Davis, T.N., 1977. Pulsating aurora: local and global morphology. *Journal of Geophysical Research* 82, 4720.
- Sandahl, I., 1985. Pitch angle scattering and particle precipitation in a pulsating aurora: an experimental study. KGI Report 185, Kiruna Geophysical Institute, Kiruna, Sweden.
- Sato, N., Morooka, M., Minatoya, K., Saemundsson, T., 1998. Nonconjugacy of pulsating auroral patches near $L = 6$. *Geophysical Research Letters* 25, 3755–3758.
- Sato, N., Wright, D.M., Ebihara, Y., Sato, M., Murata, Y., Doi, H., Saemundsson, T., Milan, S.E., Carlson, M.L.C.W., 2002. Direct comparison of pulsating aurora observed simultaneously by the FAST satellite and from the ground at Syowa. *Geophysical Research Letters* 29, 2041.
- Sato, N., Wright, D.M., Carlson, C.W., Ebihara, Y., Sato, M., Saemundsson, T., Milan, S.E., Lester, M., 2004. Generation region of pulsating aurora obtained simultaneously by the fast satellite and a Syowa–Iceland conjugate pair of observatories. *Journal of Geophysical Research* 109, 10201.
- Semeter, J., Kamalabadi, F., 2005. Determination of primary electron spectra from incoherent scatter radar measurements of the auroral E region. *Radio Science* 40, 2006.
- Smith, M.J., Bryant, D.A., Edwards, T., 1980. Pulsations in auroral electrons and positive ions. *Journal of Atmospheric and Terrestrial Physics* 42, 167.
- Stenbaek-Nielsen, H.C., 1980. Pulsating aurora: the importance of the ionosphere. *Geophysical Research Letters* 7 (5), 353.
- Stenbaek-Nielsen, H.C., Hallinan, T.J., 1979. Pulsating auroras: evidence for noncollisional thermalization of precipitating electrons. *Journal of Geophysical Research* 84, 3257.
- Störmer, C., 1948. Statistics of heights of various auroral forms from southern Norway second communication. *Journal of Geophysical Research* 53, 251–264.
- Vallance Jones, A., 1974. *Aurora*. D. Reidel, Boston, MA.
- Wahlund, J.E., Opgenoorth, H.J., Rothwell, P., 1989. Observations of thin auroral ionization layers by EISCAT in connection with pulsating aurora. *Journal of Geophysical Research* 94, 17223.
- Watanabe, M., Kadokura, A., Sato, N., Saemundsson, T., 2007. Absence of geomagnetic conjugacy in pulsating auroras. *Geophysical Research Letters* 34, 15107.
- Williams, J.D., Macdonald, E., McCarthy, M., Peticolas, L., Parks, G.K., 2006. Parallel electric fields inferred during a pulsating aurora. *Annales Geophysicae* 24, 1829–1837.
- Yamamoto, T., 1988. On the temporal fluctuations of pulsating auroral luminosity. *Journal of Geophysical Research* 93, 897.
- Yau, A.W., Whalen, B.A., McEwen, D.J., 1981. Rocket-Borne measurements of particle pulsation in pulsating aurora. *Journal of Geophysical Research* 86, 5673.